

Numerical investigation of condensation of gasoline vapor with turbulent flow in vertical tubes

Zhao Zhiwei Du Kai

(School of Energy and Environment, Southeast University, Nanjing 210096, China)

Abstract: To investigate the characteristics of the condensation in gasoline vapor condensation recovery, the condensation process of gasoline vapor with turbulent flow in a vertical tube is simulated based on the gas-liquid two-phase flow model. An effective diffusion coefficient is used to describe mass diffusion among the species of gasoline vapor. Several variables including temperature, pressure, liquid film thickness and the variation of the Nusselt number in the tube are simulated. The effects of the inlet-to-wall temperature difference and the Reynolds number on the condensation rate and the Nusselt number are obtained by modelling. The results show that heat transfer and condensation can be enhanced significantly by increasing the inlet Reynolds number. However, the increase in the inlet-to-wall temperature difference has little effect on the condensation rate. It is also found that the gasoline vapor condensation rate is influenced greatly by the mass transfer resistance. The comparison of results from the model with previous experiments shows a good agreement.

Key words: gasoline vapor; condensation; cascade refrigeration; condensation rate

Due to the significant problems caused by gasoline vapor emission, such as serious potential safety hazard, environmental pollution and energy dissipation, national standards of China^[1] have specified that the site of fuel stockpiling and transportation must have vapor recovery equipment and the vapor emission concentration should be no more than 25 g/m³. Condensation and recovery technology can liquefy and recover most of the volatile organic compounds in stages by cascade refrigeration circulation.

In the process of condensation, mass transfer of vapor is weakened by incondensable gas, which leads to a lower condensation rate. Tab. 1 shows the main constituents of gasoline vapor. It is significant to study the condensation of gasoline vapor. The process of condensation is not only influenced by the coupling of heat and mass transfer but also by multicomponent diffusion. The interaction effects can be described using the Stefan-Maxwell equation in laminar flow^[2]. Mass diffusion is influenced by both the concentration gradient and turbulent diffusion in turbulent flow. Effective diffusion coefficients were used for describing mass transport in Braun and Renz's work^[3]. Finally, the predictions reach a good agreement with experiments.

Condensation in vertical tubes is frequently encountered in industrial processes, such as gas cleaning and vapor

recovery. For condensation of vapor-gas mixture, most of the published research efforts are concerned with the geometry of vertical tubes because of their obvious relevance to many practical applications. Yu and Ma^[4] used the $k-\varepsilon$ model to describe vapor-gas mixture condensation in a turbulent tube, but low Reynolds number effects nearby the wall were not considered. In the following sections, the renormalization group(RNG) $k-\varepsilon$ model^[5] is used, which accounts for the low Reynolds number effects. The effective diffusion coefficients are also used to describe mass diffusion.

Tab. 1 Main constituents of gasoline vapor	
Constituent	Mass fraction
N ₂	0.374
O ₂	0.090
H ₂ O	0.005
C ₃ H ₆	0.003
C ₃ H ₈	0.005
C ₄ H ₈	0.177
C ₄ H ₁₀	0.097
C ₅ H ₁₂	0.215
C ₆ H ₁₄	0.034

1 Mathematical Model

1.1 Problem description

The problem considered is shown schematically in Fig. 1. A downward turbulent flow of a vapor-gas mixture enters a vertical tube of radius r_o with uniform temperature T_{in} , axial velocity u_{in} , pressure P_{in} and gas mass fraction $y_{in,i}$. The inlet pressure P_{in} is maintained at 101.325 kPa. The inlet temperature T_{in} is the saturation temperature of the mixture. The temperature of tube wall T_{wall} is maintained lower than that at the inlet. The thickness of liquid film, δ , increases along the length of the tube. The flow is assumed to be axisymmetric due to the vertical orientation of the tube and uniform inlet conditions.

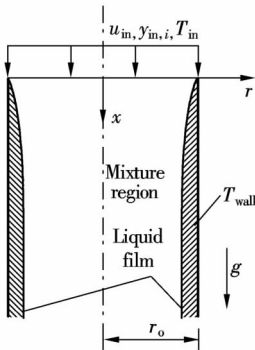


Fig. 1 Domain definition

Received 2009-11-24.
Biographies: Zhao Zhiwei (1985—), male, graduate; Du Kai (corresponding author), male, professor, du-kai@seu.edu.cn.
Citation: Zhao Zhiwei, Du Kai. Numerical investigation of condensation of gasoline vapor with turbulent flow in vertical tubes[J]. Journal of Southeast University (English Edition), 2010, 26(2): 302 – 306.

1.2 Governing equations

In formulating the governing conservation equations, it is assumed that the flow is steady, and the liquid and the mixture are Newtonian fluids. The pressure is assumed to be constant across the tube (i. e., $\partial P / \partial r = 0$), and the slip velocity between the gas phase and the liquid phase is assumed to be zero^[4]. The governing equations are as follows:

$$\frac{\partial}{\partial x}(\rho_M u_M) + \frac{\partial}{\partial r}(\rho_M v_M) = 0 \quad (1)$$

$$\begin{aligned} \frac{\partial}{\partial x}(\rho_M u_M u_M) + \frac{1}{r} \frac{\partial}{\partial r}(\rho_M v_M v_M) = \\ \frac{1}{r} \frac{\partial}{\partial r} \left(r \mu_{\text{eff}, M} \frac{\partial u_M}{\partial r} \right) + \rho_M g - \frac{dP}{dx} \end{aligned} \quad (2)$$

$$\begin{aligned} \frac{\partial}{\partial x}(\rho_M u_M C_{p, M} T) + \frac{1}{r} \frac{\partial}{\partial r}(\rho_M v_M C_{p, M} T) = \\ \frac{1}{r} \frac{\partial}{\partial r} \left(r \lambda_{\text{eff}} \frac{\partial T}{\partial r} \right) + S_E \end{aligned} \quad (3)$$

$$\frac{\partial}{\partial x}(\rho_L u_L y_L) + \frac{1}{r} \frac{\partial}{\partial r}(\rho_L v_L y_L) = S_L \quad (4)$$

$$\begin{aligned} \frac{\partial}{\partial x}(\rho_i u_i y_i) + \frac{1}{r} \frac{\partial}{\partial r}(\rho_i v_i y_i) = \frac{\partial}{\partial x} \left[r \left(\rho_i D_{\text{eff}, i} + \frac{\mu_t}{Sc_t} \right) \frac{\partial y_i}{\partial x} \right] + \\ \frac{1}{r} \frac{\partial}{\partial r} \left[r \left(\rho_i D_{\text{eff}, i} + \frac{\mu_t}{Sc_t} \right) \frac{\partial y_i}{\partial r} \right] + S_i \end{aligned} \quad (5)$$

where x is the axial coordinate, and r is the radial coordinate; ρ_M , ρ_L and ρ_i are the densities of mixture, liquid and species i , respectively; u_M , u_L and u_i are the x -directional velocities of mixture, liquid and species i , respectively; v_M , v_L and v_i are the r -directional velocities of mixture, liquid and species i , respectively; $\mu_{\text{eff}, M}$ is the effective viscosity of the mixture; μ_t is the turbulent viscosity; g is the gravitational acceleration; P is the static pressure; $C_{p, M}$ is the specific heat of the mixture; T is the temperature of the fluid; λ_{eff} is the effective thermal conductivity; S_E , S_L and S_i are the source terms of energy, liquid and species i , respectively; y_L and y_i are the mass fractions of the liquid and species i , respectively; $D_{\text{eff}, i}$ is the effective diffusion coefficient of species i ; Sc_t is the turbulent Schmidt number.

Eqs. (1) to (3) govern the conservations of mass, momentum and energy for the gas-liquid two-phase flow. Eq. (4) is the continuity equation of the liquid phase, and Eq. (5) is the mass diffusion conservation equation for the gas phase species. The effective viscosity and the thermal conductivity in both phases are defined as follows:

$$\mu_{\text{eff}} = \mu + \mu_t$$

$$\lambda_{\text{eff}} = \lambda + \lambda_t$$

where $\lambda_t = \mu_t C_p / Pr_t$; C_p is the specific heat and Pr_t is the effective Prandtl number; μ_{eff} and μ are the effective viscosity and the viscosity, respectively; λ and λ_t are the thermal conductivity and the turbulent thermal conductivity, respectively.

The effective diffusivity in the gas phase is defined as fol-

lows:

$$D_{\text{eff}} = D + D_t$$

where $D_t = \mu_t / (\rho Sc_t)$; D_{eff} , D and D_t are the effective diffusion coefficient, the diffusion coefficient and the turbulent diffusion coefficient, respectively. Pr_t and Sc_t are set equal to unity in both phases.

Phase equilibrium of gasoline vapor is described by Konovalov's first law as follows:

$$\frac{n_{g, i} - n_{\text{con}, i}}{\sum_{j=0}^8 (n_{g, j} - n_{\text{con}, j})} P = \frac{n_{L, i} + n_{\text{con}, i}}{\sum_{j=0}^6 (n_{L, j} + n_{\text{con}, j})} P_{\text{sat}, i} \quad (6)$$

where $P_{\text{sat}, i}$ is the saturation pressure; $n_{\text{con}, i}$, $n_{\text{con}, j}$ are the condensed amounts of substance; $n_{g, i}$, $n_{g, j}$ are the amounts of substance in the gas phase; $n_{L, i}$, $n_{L, j}$ are the amounts of substance of liquid phase. Omitting the minterm, the amount of substance liquefied can be expressed as

$$\begin{aligned} n_{\text{con}, i} = \\ \frac{n_{g, j} P \sum_{j=0}^6 n_{L, j} - n_{L, i} P_{\text{sat}, i} \sum_{j=0}^8 n_{g, j} + (n_{g, i} P + n_{L, i} P_{\text{sat}, i}) \sum_{j=0}^6 n_{\text{con}, j}}{P \sum_{j=0}^6 n_{L, j} + P_{\text{sat}, i} \sum_{j=0}^8 n_{g, j} + (P - P_{\text{sat}, i}) \sum_{j=0}^6 n_{\text{con}, j}} \end{aligned} \quad (7)$$

And the source terms in Eqs. (3) to (5) are

$$S_i = n_{\text{con}, i} M_i$$

$$S_L = - \sum_{i=0}^6 S_i$$

$$S_E = - \sum_{i=0}^6 S_i h_{v, i}$$

where M_i is the molecular weight, and $h_{v, i}$ is the latent heat of vaporization.

1.3 Turbulence models

In the RNG k - ε model, the turbulent viscosity is determined from the solution of the transport equations for the turbulent kinetic energy and the dissipation rate. One of the benefits of this model is that it provides an analytically-derived differential formula for effective viscosity, which accounts for low Reynolds number effects of the near-wall region. With an appropriate treatment of the near-wall region, it can be applied right up to the near-wall region and the mixture region. The transport equations are shown in Yakhot and Orszag's work^[5].

1.4 Boundary conditions

The boundary conditions for Eqs. (1) to (5) and the turbulent transport equations are as follows:

The tube wall ($r = r_o$),

$$u_M = u_i = v_M = v_i = k_M = \varepsilon_M = 0$$

The center line ($r = 0$),

$$\frac{\partial u_M}{\partial r} = \frac{\partial u_i}{\partial r} = \frac{\partial T_M}{\partial r} = \frac{\partial k_M}{\partial r} = \frac{\partial \varepsilon_M}{\partial r} = 0, \quad v_M = 0$$

where k is the turbulent kinetic energy, and ε is the dissipation rate.

At the inlet, the uniform profiles of u , T , P and y_i are specified based on actual projects, and v is set to zero. When the k - ε model is used, a uniform k inlet profile is specified using $k = 1.5 I^2 u_{in}^2$, where $I = 0.037$ in this study. A uniform inlet profile for ε is computed using $\varepsilon = k^{3/2} / (0.6 r_o)$. On the boundary of the tube wall, u , k and ε are computed using the wall function method^[6].

2 Numerical Solution Method

A transformation of coordinates is made, and the x - r coordinates are transformed into χ - η coordinates using

$$\chi = x \quad \text{for all } x \quad (8)$$

$$\eta = \begin{cases} \frac{r_o - r}{\delta} & r_o - \delta \leq r \leq r_o \\ 2 - \frac{r}{r_o - \delta} & 0 \leq r \leq r_o - \delta \end{cases} \quad (9)$$

The grid is defined with a nodal distribution of 3 000 nodes in the axial direction for a tube length of 3 m, 100 nodes in the radial direction for a tube radius of 15 mm. Nodes in the radial direction are nonuniform; the nodes in the near-wall region are intensive. QUICK schemes are used to discrete the transport equations, and the SIMPLEC method^[7] is applied for pressure-velocity coupling. Convergence is declared when the residual error is less than 1×10^{-5} for all field values.

3 Model Validations

For validations of the numerical approach, the results of the presented model are compared with those from Webb and Sardesai's^[8] experimental studies. Similar to the object of this paper, the vapor-gas mixture in Webb and Sardesai's experiment consisted of water, isopropyl alcohol and nitrogen, which entered a tube at a low temperature, and condensation took place in the tube. The boundary conditions of the model are prescribed with those of the experiments^[8].

The eight cases from Webb and Sardesai's experiments are chosen for comparison. The comparison between the outlet condensate flow rate (condensation rate) using the presented numerical model and the experimental results is shown in Fig. 2(a). For these eight cases, the predictions of the condensation rate are within $\pm 15\%$ of the experimental results. Through the comparison between the numerical values and the experimental results for the temperature differences between the inlet and outlet, it can be seen from Fig. 2(b) that the presented model produces an agreement with 85% of the numerical data being within $\pm 20\%$ of the experimental data. Overall, the model predictions show a reasonably good agreement with the experiments.

4 Results and Discussion

For gasoline vapor, results are obtained for four inlet-to-wall temperature differences ($\Delta T = 15, 25, 35, 50$ K) and four inlet Reynolds numbers ($Re_{in} = 1\,200, 1\,800, 2\,400,$

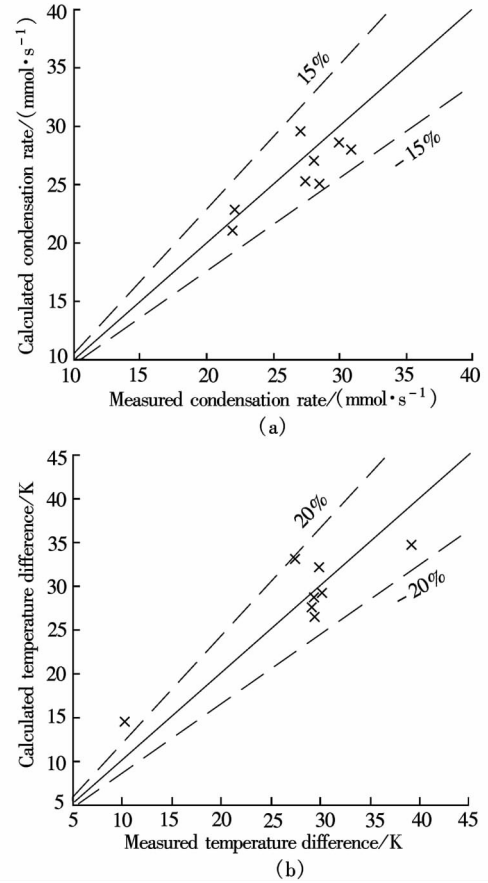


Fig. 2 Comparisons between predicted and measured data. (a) Condensation rate; (b) Inlet-to-outlet temperature difference

3 000), when the inlet temperature is set at 253.15 K as the saturation temperature of gasoline vapor. The results presented here include the detailed profiles of temperature, film thickness, pressure, and the Nusselt number along the condensation path.

4.1 Common behavior

The results obtained in this study are found to follow a common behavior for all inlet conditions. This behavior is illustrated in Fig. 3, which corresponds to gasoline vapor at the inlet conditions of $Re_{in} = 1\,200$ and $\Delta T = 25$ K.

Fig. 3(a) shows the profiles of dimensionless temperature $T^* = (T - T_{wall}) / (T_{in} - T_{wall})$ in liquid and mixture regions at various axial locations. The temperature decreases continuously in the flow direction. The T^* profiles across the liquid region are fairly close to a linear shape, which indicates that the convection terms in the energy equation are not very significant. The slope ($\partial T^* / \partial \eta^*$) at the interface of the liquid and mixture regions decreases continuously along dimensionless axial coordinate $x^* = x / (2r_o)$, which indicates a decreasing rate of heat transfer along the condensation path. Due to the heat transfer resistance of the gas boundary layer, T^* of gas phase has a sharp variation nearby the interface.

The development of liquid film thickness along x^* is illustrated in Fig. 3(b). Since the condensable components occupy a small fraction of gasoline vapor, the liquid film is very thin. The dimensionless film thickness $\delta^* = \delta / r_o$ increases while $\partial \delta^* / \partial x^*$ decreases continuously with x^* , and

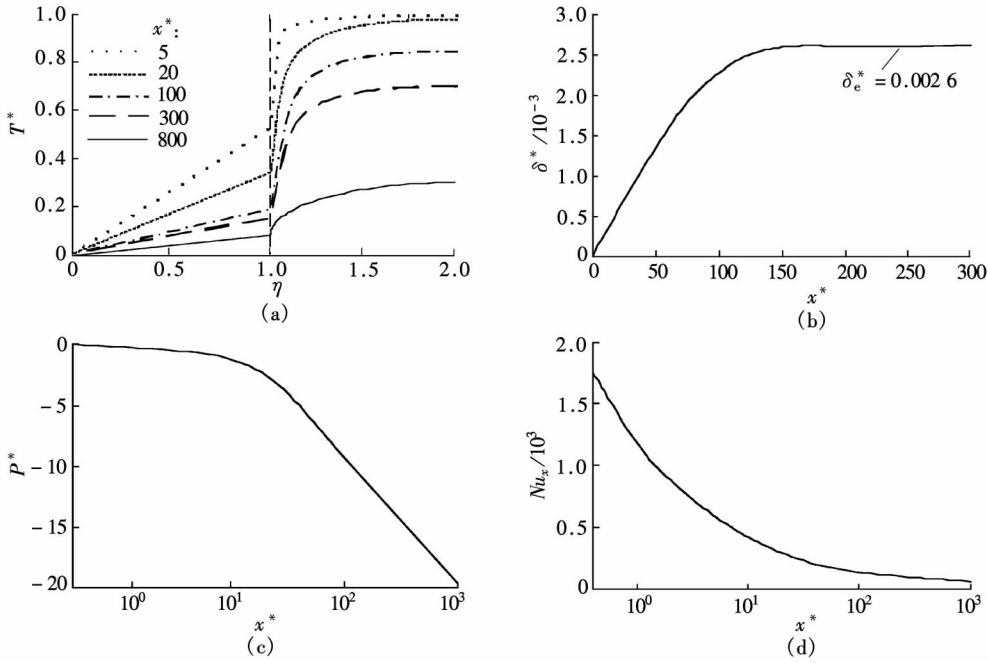


Fig. 3 Results at $Re_{in} = 1\,200$ and $\Delta T = 25$ K. (a) Temperature profiles; (b) Liquid film thickness; (c) Pressure; (d) Local Nusselt number

δ^* at the end of the condensation path, δ_e^* , reaches 0.002 6 at $x^* = 150$. The outlet δ represents the condensation rate.

The axial variations of dimensionless pressure P^* ($= (P - P_{in}) / (1/2 \rho_{in} u_{in}^2)$) are shown in Fig. 3(c). The static pressure variation is the sum of two components: a positive component due to the loss of momentum associated with the condensation process and a negative component due to the friction at the wall of the tube. The sum of these two components is ignored at all x^* under the flow conditions corresponding to Fig. 3(c). At the end of the condensation path, the momentum component disappears and the frictional component becomes invariant along x^* .

The local Nusselt number Nu_x is shown in Fig. 3(d). As expected, Nu_x decreases rapidly along x^* and approaches zero at $x^* = 100$. This rapid decrease in Nu_x is caused by the combined effects of a continuous decrease in liquid temperature and a continuous increase in δ along x^* .

The above results for gasoline vapor correspond to a particular combination of the independent variables (Re_{in} and ΔT). Effects of these independent variables on the values of δ^* and Nu_x are given in the following sections.

4.2 Effects of Re_{in} on thickness and local Nusselt number

The effects of Re_{in} on condensation parameters are investigated at $\Delta T = 25$ K. Fig. 4(a) shows the effect of Re_{in} on the film thickness δ^* . It can be found that δ_e^* and the tube length required for complete condensation increase as Re_{in} increases. The increase of δ_e^* is not only the cause of the increased inlet flow rate but also the enhancement of heat and mass transfer.

The effects of Re_{in} on heat transfer are presented in Fig. 4(b). It is shown that with the increase of Re_{in} , heat transfer is significantly enhanced, especially when x^* is between 0 and 100. It is also shown that the increase of Re_{in} has a positive effect on heat transfer, especially when x^* is between 0 and 100.

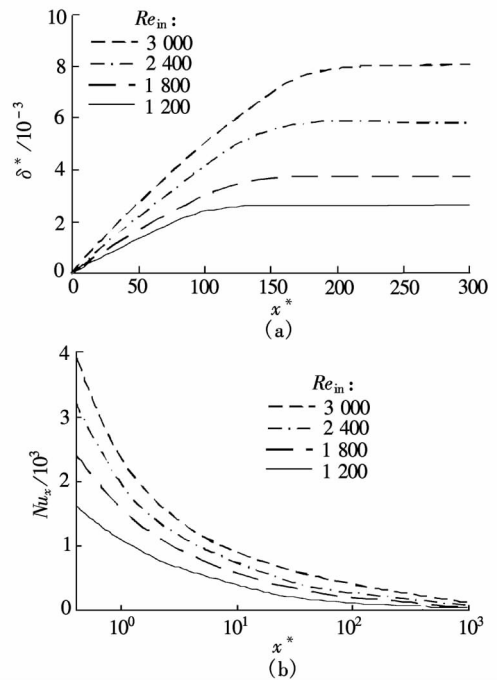


Fig. 4 Effects of Re_{in} on the results. (a) Liquid film thickness; (b) Local Nusselt number

4.3 Effects of ΔT on thickness and local Nusselt number

The effects of ΔT on the condensation parameters are investigated at $Re_{in} = 1\,200$, and the results are shown in Figs. 5(a) and (b).

Fig. 5(a) shows the effect of ΔT on δ^* at $Re_{in} = 1\,200$. It is clear that the increasing ΔT leads to increasing $\partial \delta^* / \partial x^*$ and decreasing condensation length. These trends suggest that an increase in heat flux is associated with the increase in ΔT . But the value of δ_e^* does not increase markedly as ΔT increases. This trend suggests that the condensation is greatly obstructed by the mass transfer resistance of incondensable gas; the negative effect of incondensable gas counteracts the

positive effect of increasing ΔT .

Fig. 5(b) shows the effect of ΔT on Nu_x . These results show that Nu_x decreases at any value of x^* as ΔT increases. A similar trend exists in the classical Nusselt's solution^[9] for the film condensation of pure vapors on vertical plates. In spite of the decrease in Nu_x , the wall heat flux is found to increase with ΔT . For example, for $x^* = 0$ to $x^* = 100$, the overall rate of heat transfer increases by about 22% as ΔT increases from 15 to 25 K, and a further increase of about 40% occurs as ΔT increases from 15 to 45 K.

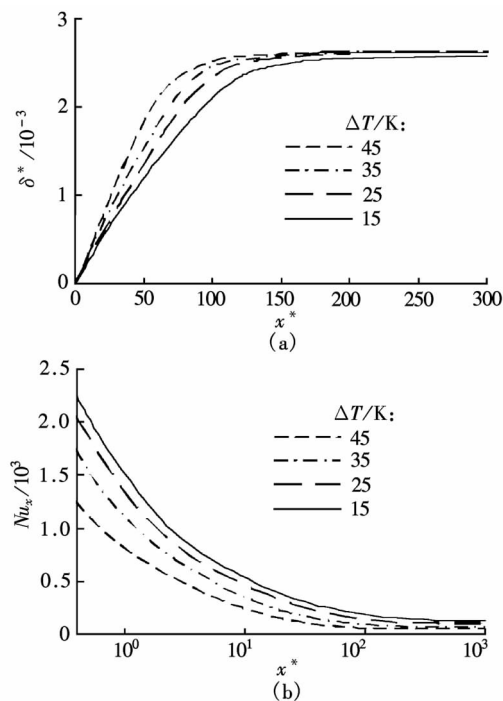


Fig. 5 Effects of ΔT on the results. (a) Liquid film thickness; (b) Local Nusselt number

5 Conclusion

Detailed numerical results are obtained regarding the condensation of gasoline vapor inside vertical tubes. The results include local profiles of temperature, as well as axial variations of the liquid film thickness, pressure, and the Nusselt

number. For a gasoline vapor condenser, the inlet Reynolds number Re_{in} and inlet-to-wall temperature difference ΔT are important independent inlet variables. Wide ranges of independent variables are covered. The effects of different variables on the condensation results are presented and discussed.

It is found that the increasing Re_{in} enhances heat and mass transfer, thus leading to the rise in the condensation rate. The increase in Re_{in} is a good approach to increasing the condensation efficiency of gasoline vapor.

The increase in ΔT leads to the increase in heat transfer, but the increase has little effect on the condensation rate. It indicates that condensation is greatly obstructed by the mass transfer resistance of incondensable gas.

References

- [1] State Environmental Protection Administration. GB 20952—2007 Emission standard of air pollutant for gasoline filling stations [S]. Beijing: China Environmental Science Press, 2007. (in Chinese)
- [2] Baumann W W, Thiele F. Heat and mass transfer in evaporating two-component liquid film flow [J]. *Int J Heat Mass Transfer*, 1990, **33**(2): 267–273.
- [3] Braun M, Renz U. Multicomponent diffusion interactions during condensation in laminar and turbulent pipe flow [J]. *Int J Heat Mass Transfer*, 1997, **40**(1): 131–139.
- [4] Yu Hui, Ma Kongjun, Zhu Jiahua, et al. Fogging and filming of high humidity gas flow under effect of cooling surface [J]. *Journal of Chemical Industry and Engineering*, 2006, **157**(18): 1897–1903. (in Chinese)
- [5] Yakhot V, Orszag S A. Renormalization group analysis of turbulence: basic theory [J]. *Journal of Scientific Computing*, 1986, **1**(1): 3–11.
- [6] Launder B E, Spalding D B. Numerical computation of turbulent flows [J]. *Computer Methods Applied Mechanics Eng*, 1974, **3**(2): 269–289.
- [7] Versteeg H K, Malalasekera W. *An introduction to fluid dynamic* [M]. Essex, UK: Addison Wesley Longman Ltd, 1995.
- [8] Webb D R, Sardesai R G. Verification of multicomponent mass transfer models for condensation [J]. *International Journal of Multiphase Flow*, 1981, **7**(5): 507–520.
- [9] Nusselt W. Die oberflächen kondensation des wasserdampfes [J]. *Z Detsch Ing*, 1916, **60**: 541–546.

油气在竖直管内湍流流动时冷凝的数值模拟

赵志伟 杜 垚

(东南大学能源与环境学院, 南京 210096)

摘要: 为了探索油气在冷凝回收过程中的冷凝规律, 采用气液两相流模型描述了油气在竖直管内湍流流动时的冷凝过程. 采用有效传质系数描述了油气组分的质量传递. 模拟了油气在管内冷凝时的温度、管内压力、液膜厚度和 Nusselt 数的变化, 得到了入口油气和管壁的温差、雷诺数对冷凝率和 Nusselt 数的影响. 结果显示: 增大入口雷诺数能显著增强传热和冷凝, 但是增大入口油气和管壁的温差对冷凝率的影响较小; 另外, 还发现传质阻力对油气冷凝率有较大影响. 此模型的计算结果与先前的实验数据能够很好地符合.

关键词: 油气; 冷凝; 复叠制冷; 冷凝率

中图分类号: TE85